# Multi-storey Building Retrofit by ADAS-Equipped Braces

Terenzi Gloria[1(✉)], Sorace Stefano[2], Melani Damiano[3], and Fuso Elena[2]

[1] Department of Civil and Environmental Engineering, University of Florence, 50139 Florence, Italy
gloria.terenzi@unifi.it
[2] Polytechnic Department of Engineering and Architecture, University of Udine, 33100 Udine, Italy
{stefano.sorace,elena.fuso}@uniud.it
[3] Department of Civil and Environmental Engineering, University of Florence, 50139 Florence, Italy
damiano.melani@stud.unifi.it

**Abstract.** An alternative passive energy-based retrofit design is proposed for a reinforced concrete building, seismically retrofitted in 2013 and damaged by the 2016 Central Italy earthquake. An evaluation analysis carried out by referring to the pre-2013 conditions shows unsafe stress states in most structural members and severe damage in the masonry partitions and perimeter infills. The alternative retrofit strategy of the building, which consists in the incorporation of a dissipative bracing system equipped with pressurized fluid viscous spring-dampers, allows attaining a substantial seismic performance improvement. This is assessed by a safe response of all columns and beams, and at most a very slight damage in the masonry panels, in post-intervention conditions.

**Keywords:** ADAS dampers · Energy-based design · Seismic assessment · Seismic retrofit · Frame buildings · Reinforced concrete structures

## 1 Introduction

Incorporation of dissipative bracing systems is an emerging seismic retrofit strategy for frame structures. Among the several types of devices currently adopted as passive protection elements, Added Damping and Stiffness (ADAS) steel dissipaters have a well-established tradition [1–3]. This is a consequence of their plain working principle, based on the elastic-plastic behaviour of the constituting plates, as well as of their relatively easy installation. In spite of this, the design of ADAS dampers is not simple, because it requires a proper balance between the addition of energy dissipation and horizontal translational stiffness. The former allows remarkably reducing the plastic demand on the structural members. The latter is always beneficial in terms of lateral displacements but, as long as the dampers respond elastically, it causes a significant increase in base shear, and thus in the stress states of the frame elements and the foundations.

In view of this, an energy-based pre-sizing criterion of dampers was recently proposed by the first two authors [4, 5], aimed at achieving a joined control of stress states and displacements. According with this criterion, the total number of plates constituting ADAS devices is tentatively fixed by: a. pre-estimating the energy dissipation capable of providing a target drop of base shear in retrofitted conditions; b. computing the energy dissipation by assuming a maximum displacement of the dissipaters calibrated on a target reduction of storey drifts.

In this paper a new energy-based pre-sizing procedure is formulated, where the energy dissipation capacity of the dampers is evaluated by expressly taking into account the reduction of the fundamental vibration period of the structure caused by the bracing system-related increase of horizontal stiffness.

This new sizing criterion is demonstratively applied to a representative case study, i.e. a 6-storey residential building with reinforced concrete structure situated in the municipality of L'Aquila, Abruzzo, Italy. Based on the results of a seismic assessment analysis initially carried out, three different installations of the ADAS dissipaters in plan and along the height of the building are comparatively examined, with the aim of providing practical suggestions for the best placement of the protective system for target performance levels.

## 2 Case-Study Building

The case study building is located in L'Aquila, Abruzzo, Italy, and was designed according with the 1986 edition of the Italian Seismic Standards. It has a (21.05 × 11.45) m$^2$ sized rectangular plan (Fig. 1, referred to the lower three storeys), and is articulated in six above-ground storeys, with inter-storey heights equal to 3.4 m (first storey) and 3.04 m (remaining ones).

The structure is constituted by a reinforced concrete frame skeleton. Columns have the following cross sections: 600 × 300 mm$^2$ (highlighted in red in Fig. 1), 550 × 300 mm$^2$ (blue), 500 × 300 mm$^2$ (green) and 400 × 300 mm$^2$ (black) on the three lower storeys, and 300 × 300 mm$^2$, on the three upper storeys. Perimeter beams have out-of-depth sections sized 300 × 500 mm$^2$, and internal beams have in-depth sections sized 800 × 300 mm$^2$ (2–5 alignments in Fig. 1) and 600 × 300 mm$^2$ (B and C alignments), at all floors.

A view of the finite element model of the structure, generated by SAP2000NL software [6], is displayed in Fig. 2. A modal analysis carried out by this model highlighted two main translational modes in current state, along *X* and *Y* axis in plan, with vibration periods equal to 1.21 s and 1.18 s, and effective masses of 84% and 82.7%, respectively.

Based on the data extracted from the available technical documentation, the following mechanical properties were assumed for the materials: mean cubic compressive strength of concrete equal to 25 MPa; yield stress of the reinforcing steel bars equal to 430 MPa. These were assumed as reference values both for the finite element and stress check analyses.

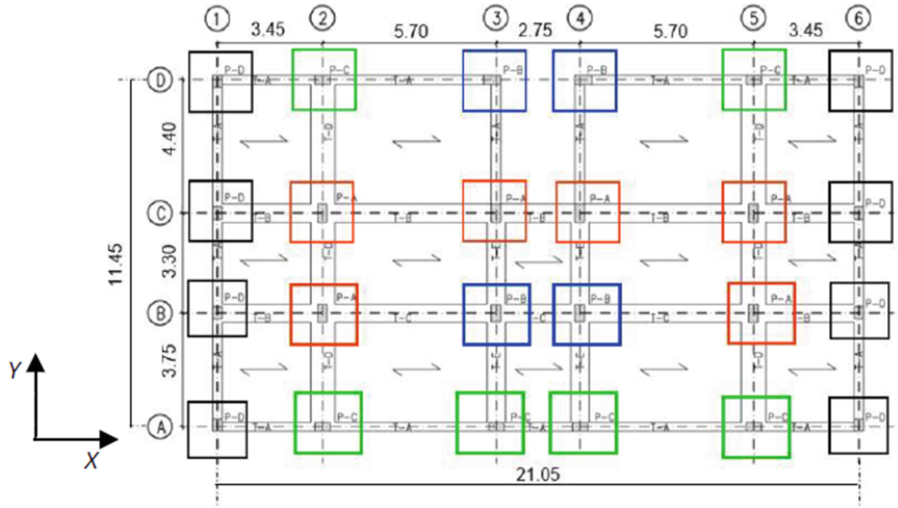


**Fig. 1.** Structural plan of the building.

## 3 Seismic Assessment of the Building

The seismic assessment study was developed via time-history analysis by using in input a set of seven accelerograms for the two axes in plan and the vertical axis, generated from the pseudo-acceleration response spectra plotted in Fig. 3. Therein, the three spectral graphs for the horizontal and vertical components are referred to the Serviceability Design Earthquake (SDE), Basic Design Earthquake (BDE) and Maximum Considered Earthquake (MCE) hazard levels, for C-type soil and T1-type topographic category. The corresponding peak ground acceleration values are: 0.156 g (SDE), 0,347 g (BDE), and 0.407 g (MCE), for the horizontal components; 0.045 g (SDE), 0.180 g (BDE) and 0.261 g (MCE), for the vertical one.

The results of the analysis in current conditions are synthesized in Tables 1 and 2. Table 1 reports the maximum storey shears along the two axes, $V_x$ and $V_y$, and their ratios, $\rho_{sx}$ and $\rho_{sy}$, to relevant strength values, $V_{xR}$ and $V_{yR}$. Table 2 lists the maximum inter-storey drifts, $u_x$ and $u_y$, and their ratios, $\rho_{ux}$ and $\rho_{uy}$, to the Immediate Occupancy drift performance limit for buildings with masonry infills and partitions, $Id_{IO}$, fixed at 0.5% of the inter-storey height $h$ by the Italian Technical Standards [7].

As shown in Table 1, $\rho_s$ ratios greater than 1 are found for the two lower storeys at the SDE and for the four lower storeys at the BDE, reaching values of about 3 for the latter. $\rho_s$ values below 1 come out only for the top storey at the MCE, the maximum values for which are equal to 3.66.

## 4 Dissipative Bracing-Based Retrofit—Sizing Criterion and Application to Different Design Solutions

The seismic assessment study was developed via time-history analysis by using in input a set of seven accelerograms for the two axes in plan and the vertical axis.

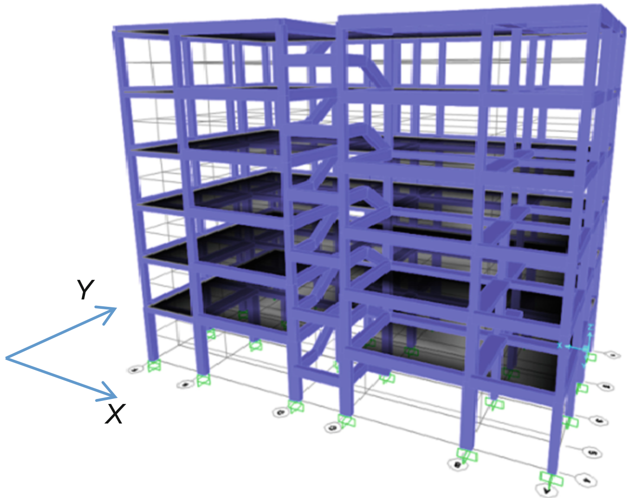


**Fig. 2.** View of the finite element model of the structure.

As mentioned in the Introduction, the retrofit hypothesis proposed herein consists in the installation of a dissipative bracing system incorporating ADAS steel dampers with triangular shape (also named T-ADAS in the literature) as protective devices. The geometry of a plate and the schematic hysteretic cycle of a damper are traced out in Fig. 4.

The preliminary sizing procedure of the dampers proposed in this study is based on a quick estimation of the protective system energy dissipation capacity by which a pre-established reduction of lateral displacements and base shear is attained. For frame structures with a substantially regular geometry in plan and elevation, this evaluation is carried out in terms of spectral quantities, by referring to the periods of the first translational modes along the two coordinate axes in plan (which a predominant portion of modal masses is associated with, in the above-mentioned hypothesis of structural regularity). Both in current and retrofitted conditions, these periods are assumed to be included in the wide period interval $T_C$-$T_D$ of the response spectra that corresponds to the constant pseudo-velocity branch, where the fundamental vibration periods of low through mid-to-high rise reinforced concrete frame structures are always situated.

For each one of the two axes in plan, named $T_{IN}$ the fundamental period in current state, the procedure starts by fixing a tentative reduction, $\Delta S_{D\text{-}}$, of the spectral displacement $S_D$ computed for $T_{IN}$. Then, named $S_{V,cost}$ the value of the horizontal branch of the pseudo-velocity spectrum, the period in retrofitted conditions, $T_{FIN}$, given by the difference between $T_{IN}$ and the period reduction $\Delta T$ caused by $\Delta S_{D\text{-}}$, can be evaluated as follows:

$$T_{FIN} = T_{IN} - \Delta T = T_{IN} - \frac{2\pi \, \Delta S_D}{S_V} \tag{1}$$

As illustrated in Fig. 5, a rise ($\Delta S_{A+}$) in the initial pseudo-acceleration ordinate comes out when passing from $T_{IN}$ to $T_{FIN}$, as a consequence of the stiffening effect of

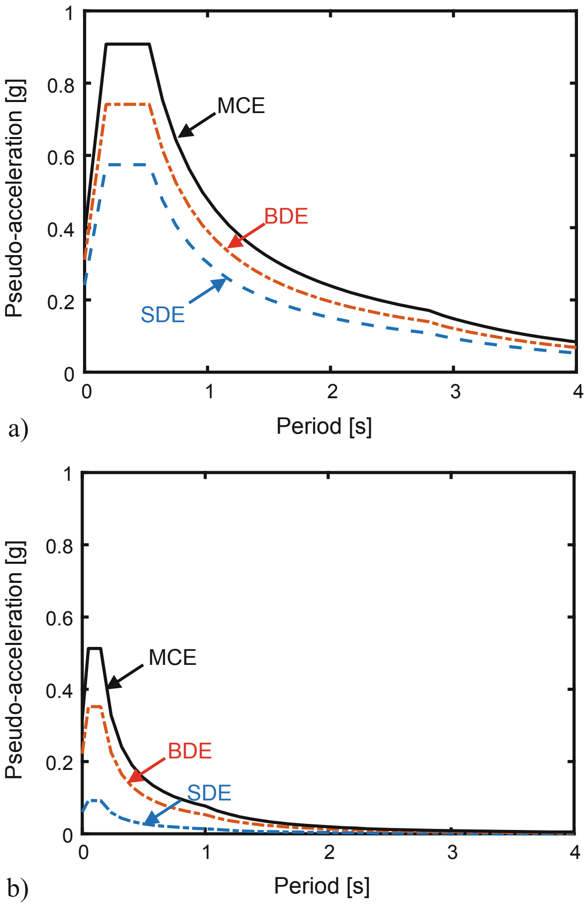


**Fig. 3.** Horizontal (a) and vertical (b) pseudo-acceleration elastic response spectra for L'Aquila—SDE, BDE and MCE hazard levels.

the dissipative bracing system. The supplemental damping contribution of the latter must guarantee a drop in the spectral ordinate, $\Delta S_{A\text{-},diss}$, significantly exceeding $\Delta S_{A+}$ and capable of reaching the target $S_A(T_{FIN})$ value in retrofitted conditions. The corresponding reduction in base shear, $\Delta V$, is obtained by multiplying $\Delta S_{A\text{-},diss}$ by the seismic mass $M$ of the building.

Hence, the tentative energy dissipation capacity to be assigned to the protective system is computed as:

$$E_D = 4\Delta V \Delta S_D \tag{2}$$

Based on the values calculated by Eq. (2) for the two axes in plan, $E_{d,x}$, $E_{d,y}$, the corresponding total numbers of plates, $n_{p,x}$, $n_{p,y}$, are evaluated by dividing $E_{d,x}$, $E_{d,y}$ by the maximum energy that each plate can dissipate in a cycle bounded by the maximum estimated displacement, $E_{d,pl}$, multiplied by 11 to take into account also the energy dissipated in the remaining cycles, characterized by smaller amplitudes [4, 8]. In the

**Table 1.** Current conditions: maximum storey shear and $\rho_S$ values.

| Storey | S1 | S2 | S3 | S4 | S5 | S6 |
|---|---|---|---|---|---|---|
| $V_{xR}$ (kN) | 1996 | 1814 | 1667 | 1696 | 1696 | 1696 |
| $V_{yR}$ (kN) | 2337 | 1912 | 1813 | 1696 | 1696 | 1696 |
| *SDE* | | | | | | |
| $V_x$ (kN) | 2772 | 1846 | 1485 | 1157 | 827 | 378 |
| $V_y$ (kN) | 2571 | 1520 | 1379 | 1949 | 752 | 374 |
| $\rho_{sx}$ | 1.39 | 1.02 | 0.89 | 0.68 | 0.42 | 0.22 |
| $\rho_{sy}$ | 1.10 | 0.79 | 0.76 | 0.62 | 0.44 | 0.22 |
| *BDE* | | | | | | |
| $V_x$ (kN) | 5967 | 4245 | 3155 | 2419 | 1638 | 725 |
| $V_y$ (kN) | 6193 | 3654 | 3288 | 2531 | 1664 | 767 |
| $\rho_{sx}$ | 2.99 | 2.34 | 1.89 | 1.43 | 0.96 | 0.43 |
| $\rho_{sy}$ | 2.65 | 1.91 | 1.81 | 1.49 | 0.98 | 0.45 |
| *MCE* | | | | | | |
| $V_x$ (kN) | 7315 | 5259 | 3934 | 3002 | 2053 | 590 |
| $V_y$ (kN) | 7383 | 4403 | 3857 | 2993 | 2074 | 975 |
| $\rho_{sx}$ | 3.66 | 2.89 | 2.36 | 1.77 | 1.21 | 0.52 |
| $\rho_{sy}$ | 3.16 | 2.30 | 2.12 | 1.76 | 1.22 | 0.57 |

$E_{d,pl}$ calculation the maximum plate displacement, $d_{max}$, is tentatively put as equal to $ID_{IO}$, in order to obtain a substantial constraint of drifts up to the highest normative earthquake level considered in the analysis (BDE or MCE).

The diagonal braces are sized by evaluating the increase in lateral stiffness of the structure, $\Delta K$, related to the $\Delta T$ transition from $T_{IN}$ and $T_{FIN}$ induced by the incorporation of the protective system, as follows:

$$\Delta K = \frac{4\pi^2 M}{\Delta T^2} \tag{3}$$

For the case study application, by referring to the nomenclature in Fig. 4, the geometric sizes selected for the plates are: $H = 150$ mm, $t = 15$ mm, and $B = 75$ mm. The constituting steel is type S275, with yield stress and tensile strength equal to $f_{yk} = 275$ N/mm$^2$ and $f_{tk} = 430$ N/mm$^2$, respectively. By assuming a target $S_D(T_{FIN})$ value of the building equal to 0.5% of its total height, i.e. $S_D(T_{FIN}) = 93$ mm, by applying relations (1–3), the following demands in terms of plate numbers are computed for the two references axes:

$X$ axis—$T_{IN,x} = 1.21$ s, $S_{D,x}(T_{IN,x}) = 159.4$ mm, $S_{V,x} = 665.7$ mm/s, $\Delta S_{D\text{-},x} =$ (159.4–93) mm = 66.4 mm, $T_{FIN,x} = 0{,}583$ s, $S_{A,x}(T_{FIN,x}) = 0.723$ g, $M = 1675.4$ kN/g, $E_{d,x} = 1632.6$ KNm, $E_{d,plate,x} = 3.58$ KNm;

**Table 2.** Current conditions: maximum inter-storey drift and $\rho_u$ values.

| Storey | S1 | S2 | S3 | S4 | S5 | S6 |
|---|---|---|---|---|---|---|
| $u_R$ (mm) | 17.0 | 15.3 | 15.3 | 15.3 | 15.3 | 15.3 |
| *SDE* | | | | | | |
| $u_x$ (mm) | 13.4 | 14.4 | 13.7 | 11.7 | 7.7 | 3.6 |
| $u_y$ (mm) | 9.8 | 11.3 | 11.3 | 10.3 | 7.0 | 3.7 |
| $\rho_{ux}$ | 0.78 | 0.94 | 0.89 | 0.76 | 0.50 | 0.23 |
| $\rho_{uy}$ | 0.57 | 0.74 | 0.74 | 0.67 | 0.46 | 0.24 |
| *BDE* | | | | | | |
| $u_x$ (mm) | 28.1 | 36.9 | 41.8 | 35.5 | 24.8 | 11.2 |
| $u_y$ (mm) | 23.6 | 32.5 | 33.6 | 27.5 | 12.1 | 9.3 |
| $\rho_{ux}$ | 1.65 | 2.41 | 2.73 | 2.32 | 1.62 | 0.73 |
| $\rho_{uy}$ | 1.39 | 2.12 | 2.19 | 1.79 | 0.79 | 0.61 |
| *MCE* | | | | | | |
| $u_x$ (mm) | 34.2 | 48.0 | 47.5 | 41.2 | 31.4 | 14.6 |
| $u_y$ (mm) | 31.3 | 44.6 | 50.9 | 40.5 | 22.1 | 17.7 |
| $\rho_{ux}$ | 2.01 | 3.14 | 3.01 | 2.69 | 2.05 | 0.95 |
| $\rho_{uy}$ | 1.84 | 2.91 | 3.32 | 2.65 | 1.44 | 1.15 |

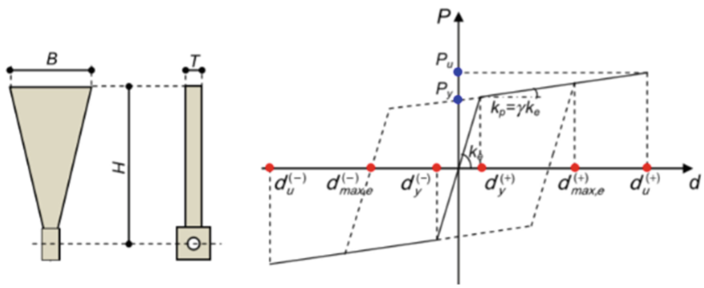


**Fig. 4.** Geometry of a triangular plate and hysteretic cycle of a device.

*Y* axis—$T_{IN,y}$ = 1.18 s; $S_{D,y}(T_{IN,y})$ = 155.4 mm, $S_{V,y}$ = 665.7 mm/s, $\Delta S_{D\text{-},y}$ = (155.4–93) mm = 62.4 mm, $T_{FIN,y}$ = 0,591 s, $S_{A,y}(T_{FIN,y})$ = 0.72 g, $E_{d,y}$ = 1481 KNm; $E_{d,plate,y}$ = 3.58 KNm.

The ratios of $E_{d,x}$ to $E_{d,plate,x}$, and $E_{d,y}$ to $E_{d,plate,y}$ result in the following numbers of plates in *X* and *Y*: $n_{px}$ = 455 and $n_{py}$ = 414. Thus, the total number of plates for the building, $n_{p,tot}$, is equal to 869.

Based on this preliminary sizing, three different installation solutions—named RS1, RS2, RS3 in the following—were designed by varying the distribution in plan and elevation of the dissipative braces, as described below. In all cases, no dampers are

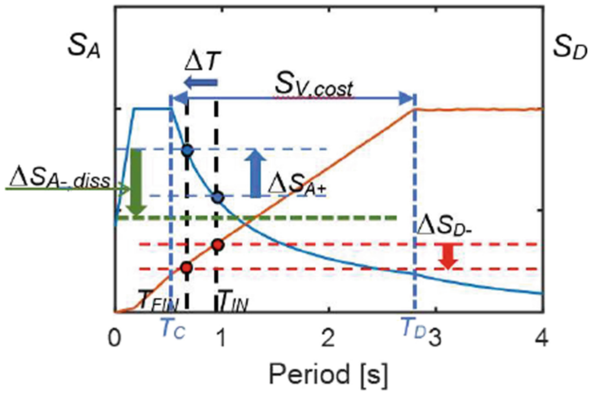


**Fig. 5.** Quantities involved in the sizing procedure.

installed on the upper floor, because of the elastic response of relevant structural members in current state up to the BDE. By complying with Eq. (3), a circular tubular section with a 150 mm diameter, 4.6 mm thick in $X$ and 3 mm thick in $Y$, was selected for the supporting steel braces.

RS1 retrofit solution. 12 plate-dampers placed in 6 bays along $X$, and 8 in $Y$, giving rise to $n_{p,x} = 360$, $n_{p,y} = 480$, and $n_{p,tot} = 840$. This choice is aimed at minimizing the architectural impact of the intervention in $X$. Figure 6 shows the positions in plan of the dissipative braces along $X$ (evidenced in yellow), and $Y$ (in red).

RS2 retrofit solution. 12 plate-dampers placed in 8 bays both along $X$ and $Y$, with $n_{p,x} = n_{p,y} = 480$, and $n_{p,tot} = 960$, nearly coinciding with the tentative plate numbers calculated by the sizing procedure.

RS3 retrofit solution. 12 plate-dampers on the first storey, 14 on the second and third, 10 on the fourth and 8 on the fifth in 8 bays for each direction, resulting in $n_{p,x} = n_{p,y} = 464$, and $n_{p,tot} = 928$. This distribution is approximately proportional to the first modal shapes of the structure in $X$ and $Y$. Figure 7 shows the positions in plan of the dissipative braces along $X$ (in yellow), and $Y$ (in red) mutually adopted for the RS2 and RS3 solutions.

### 4.1 RS1—Results

The two fundamental translational modes in $X$ and $Y$ are kept, with modified periods of 0.67 s and 0.64 s, and effective masses of 73.5% and 80.7%, respectively. The mass reductions are due to a little transfer to the torsional mode contributions caused by the asymmetric installation of the bracing system in plan (along 6 bays in $X$, and 8 in $Y$, as stated above). The results of the time-history analyses are recapitulated in Tables 3 and 4. A generalized improvement of seismic performance is observed, except for the first storey, where the energy dissipation benefits do not compensate for the response increase caused by the stiffening effects of the protective system. Moreover, the even greater benefits obtained in $X$, in spite of the lower number of plates assumed for this direction, are as a consequence of the greater amount of energy dissipated, as compared to $Y$.

**Table 3.** Retrofitted conditions—RS1: maximum storey shear and $\rho_S$ values.

| Storey | S1 | S2 | S3 | S4 | S5 | S6 |
|---|---|---|---|---|---|---|
| $V_{xR}$ (kN) | 1996 | 1814 | 1667 | 1696 | 1696 | 1696 |
| $V_{yR}$ (kN) | 2337 | 1912 | 1813 | 1696 | 1696 | 1696 |
| *SDE* | | | | | | |
| $V_x$ (kN) | 1975 | 1085 | 764 | 552 | 342 | 98 |
| $V_y$ (kN) | 2278 | 1106 | 877 | 585 | 380 | 141 |
| $\rho_{sx}$ | 0.98 | 0.59 | 0.46 | 0.32 | 0.20 | 0.06 |
| $\rho_{sy}$ | 0.97 | 0.58 | 0.48 | 0.34 | 0.22 | 0.08 |
| *BDE* | | | | | | |
| $V_x$ (kN) | 4689 | 2841 | 1979 | 1448 | 958 | 223 |
| $V_y$ (kN) | 5331 | 3236 | 2578 | 1725 | 1128 | 402 |
| $\rho_{sx}$ | 2.35 | 1.56 | 1.18 | 0.85 | 0.56 | 0.13 |
| $\rho_{sy}$ | 2.28 | 1.69 | 1.42 | 1.01 | 0.66 | 0.23 |
| *MCE* | | | | | | |
| $V_x$ (kN) | 6326 | 3844 | 2357 | 1917 | 1233 | 275 |
| $V_y$ (kN) | 6614 | 3797 | 3022 | 2018 | 1317 | 456 |
| $\rho_{sx}$ | 3.17 | 2.12 | 1.41 | 1.13 | 0.73 | 0.16 |
| $\rho_{sy}$ | 2.96 | 1.98 | 1.66 | 1.19 | 0.77 | 0.27 |

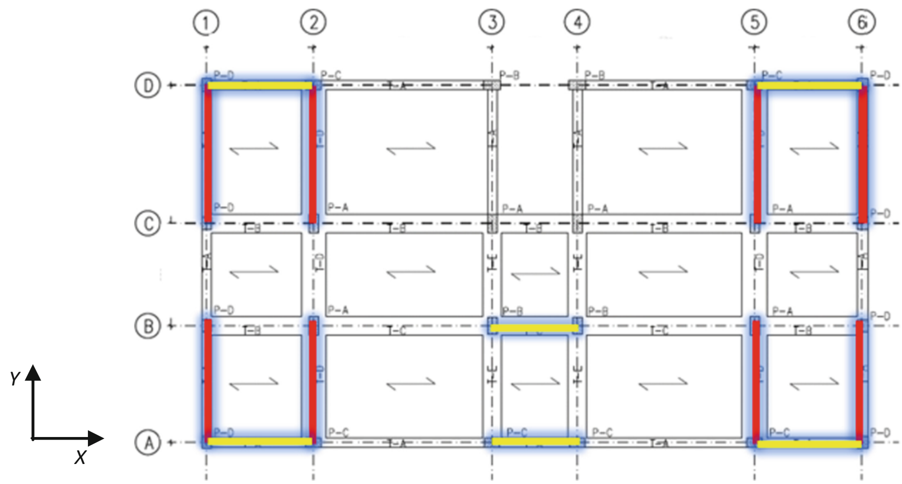


**Fig. 6.** RS1 retrofit solution: positions of the dissipative bracing system alignments in plan.

**Table 4.** Retrofitted conditions—RS1: maximum inter-storey drift and $\rho_u$ values.

| Storey | S1 | S2 | S3 | S4 | S5 | S6 |
|---|---|---|---|---|---|---|
| $u_R$ (mm) | 17.0 | 15.3 | 15.3 | 15.3 | 15.3 | 15.3 |
| *SDE* | | | | | | |
| $u_x$ (mm) | 8.8 | 8.6 | 7.4 | 5.5 | 3.6 | 1.6 |
| $u_y$ (mm) | 9.6 | 9.5 | 7.9 | 6.5 | 4.8 | 2.3 |
| $\rho_{ux}$ | 0.52 | 0.56 | 0.48 | 0.36 | 0.23 | 0.10 |
| $\rho_{uy}$ | 0.56 | 0.62 | 0.52 | 0.42 | 0.31 | 0.15 |
| *BDE* | | | | | | |
| $u_x$ (mm) | 23.9 | 23.4 | 20.6 | 15.8 | 10.3 | 4.3 |
| $u_y$ (mm) | 26.6 | 26.3 | 22.1 | 18.6 | 13.5 | 6.5 |
| $\rho_{ux}$ | 1.40 | 1.53 | 1.35 | 1.03 | 0.67 | 0.28 |
| $\rho_{uy}$ | 1.56 | 1.72 | 1.44 | 1.22 | 0.88 | 0.42 |
| *MCE* | | | | | | |
| $u_x$ (mm) | 29.5 | 28.9 | 25.6 | 19.5 | 12.9 | 5.2 |
| $u_y$ (mm) | 31.5 | 31.3 | 26.2 | 21.9 | 15.9 | 7.6 |
| $\rho_{ux}$ | 1.73 | 1.88 | 1.67 | 1.27 | 0.84 | 0.33 |
| $\rho_{uy}$ | 1.85 | 2.04 | 1.71 | 1.43 | 1.04 | 0.49 |

### 4.2 RS2—Results

The two fundamental translational modes in $X$ and $Y$ have periods of 0.622 s and 0.619 s in $X$ and $Y$, and effective masses of 72.2% and 76.5%, respectively, highlighting small reductions as compared to the RS1 solution, but virtually equal values of periods and closer values of masses for the two axes.

As highlighted in Tables 5 and 6, the time-history response in terms of stress states is virtually coincident with the RS1 one in $Y$, whereas it is slightly decreased (SDE), increased (BDE), or very similar (MCE), in $X$. At the same time, drifts are lowered up to about 10% in $Y$ and 15% in $X$.

### 4.3 RS3—Results

The two fundamental translational modes have periods of 0.621 s and 0.618 s in $X$ and $Y$, and effective masses of 75.3% and 77.1%, respectively, i.e., practically coincident periods with the RS2 solution, and an about 3% increased mass in $X$ and less than 1% in $Y$, as compared to it.

As illustrated by Tables 7 and 8, the first mode-proportional distribution of dampers along the height provides, with a 3.3% smaller number of plates than for RS2, an additional regularization of the demand on the various storeys due to the highest dissipation offered by the protective system on the second and third ones, in terms both of stress states and drifts.

**Table 5.** Retrofitted conditions—RS2: maximum storey shear and $\rho_S$ values.

| Storey | S1 | S2 | S3 | S4 | S5 | S6 |
|---|---|---|---|---|---|---|
| $V_{xR}$ (kN) | 1996 | 1814 | 1667 | 1696 | 1696 | 1696 |
| $V_{yR}$ (kN) | 2337 | 1912 | 1813 | 1696 | 1696 | 1696 |
| *SDE* | | | | | | |
| $V_x$ (kN) | 1711 | 1020 | 691 | 490 | 316 | 62 |
| $V_y$ (kN) | 2262 | 1106 | 849 | 588 | 384 | 140 |
| $\rho_{sx}$ | 0.86 | 0.56 | 0.41 | 0.29 | 0.19 | 0.04 |
| $\rho_{sy}$ | 0.97 | 0.58 | 0.47 | 0.35 | 0.23 | 0.08 |
| *BDE* | | | | | | |
| $V_x$ (kN) | 5039 | 3064 | 2171 | 1572 | 1012 | 164 |
| $V_y$ (kN) | 5259 | 3233 | 2581 | 1730 | 1129 | 407 |
| $\rho_{sx}$ | 2.52 | 1.68 | 1.30 | 0.93 | 0.59 | 0.09 |
| $\rho_{sy}$ | 2.25 | 1.69 | 1.42 | 1.02 | 0.66 | 0.24 |
| *MCE* | | | | | | |
| $V_x$ (kN) | 6224 | 3757 | 2662 | 1984 | 1281 | 192 |
| $V_y$ (kN) | 6676 | 3850 | 3068 | 2049 | 1333 | 449 |
| $\rho_{sx}$ | 3.12 | 2.07 | 1.59 | 1.17 | 0.75 | 0.11 |
| $\rho_{sy}$ | 2.86 | 2.01 | 1.69 | 1.2 | 0.78 | 0.26 |

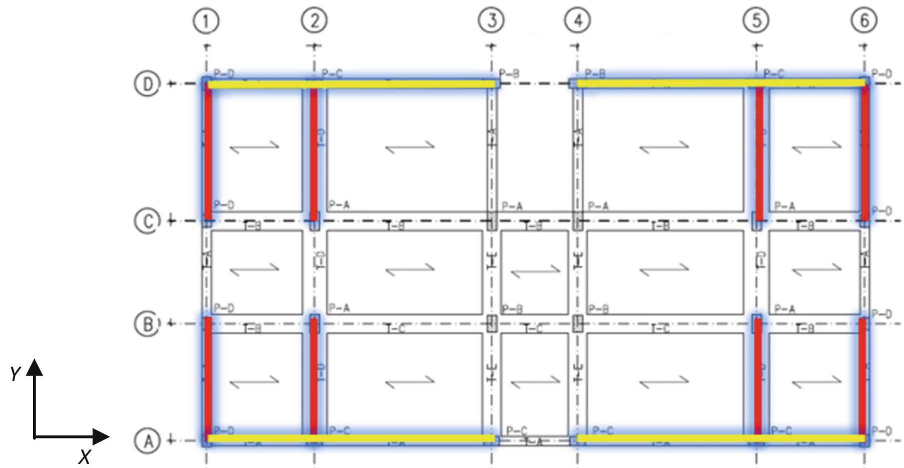


**Fig. 7.** RS2 and RS3 retrofit solutions: positions of the dissipative bracing system alignments in plan.

**Table 6.** Retrofitted conditions—RS2: maximum inter-storey drift and $\rho_u$ values.

| Storey | S1 | S2 | S3 | S4 | S5 | S6 |
|---|---|---|---|---|---|---|
| $u_R$ (mm) | 17.0 | 15.3 | 15.3 | 15.3 | 15.3 | 15.3 |
| *SDE* | | | | | | |
| $u_x$ (mm) | 7.4 | 7.1 | 6.1 | 4.4 | 2.7 | 0.9 |
| $u_y$ (mm) | 8.7 | 8.5 | 6.1 | 4.4 | 2.7 | 0.9 |
| $\rho_{ux}$ | 0.43 | 0.46 | 0.39 | 0.28 | 0.17 | 0.06 |
| $\rho_{uy}$ | 0.51 | 0.55 | 0.47 | 0.37 | 0.26 | 0.14 |
| *BDE* | | | | | | |
| $u_x$ (mm) | 21.7 | 21.5 | 18.9 | 14.0 | 8.5 | 2.5 |
| $u_y$ (mm) | 25.6 | 24.9 | 21.0 | 17.0 | 12.1 | 6.6 |
| $\rho_{ux}$ | 1.27 | 1.4 | 1.23 | 0.91 | 0.55 | 0.16 |
| $\rho_{uy}$ | 1.50 | 1.63 | 1.37 | 1.11 | 0.79 | 0.43 |
| *MCE* | | | | | | |
| $u_x$ (mm) | 26.8 | 26.4 | 23.2 | 17.6 | 10.9 | 3.1 |
| $u_y$ (mm) | 30.5 | 29.6 | 25.0 | 20.3 | 14.3 | 7.8 |
| $\rho_{ux}$ | 1.57 | 1.72 | 1.51 | 1.15 | 0.71 | 0.2 |
| $\rho_{uy}$ | 1.79 | 1.93 | 1.63 | 1.32 | 0.93 | 0.51 |

## 5 Conclusions

The energy-based sizing procedure for ADAS dampers proposed in this paper, based on simple spectral relations for the original structure, schematized like a SDOF system in the hypothesis of a substantial regularity in plan and elevation, was demonstratively applied to the seismic retrofit of a multi-storey reinforced concrete residential building.

Starting from the estimated minimum number of plates needed to reach the target performance, three different solutions for the installation of the protective system were designed and comparatively evaluated.

Although the assessed performance was similar for the three hypotheses, both in terms of stress states and inter-storey drifts, the analyses highlighted that the most effective distribution of plates is obtained by conceiving it as proportional to the lateral deformation of the original structure.

This is underlined by the RS3 retrofit solution, which complies with this concept. Indeed, although including a smaller total number of plates as compared to RS2, characterized by a uniform distribution of plates in elevation, RS3 guarantees the best combined performance, as it constrains further the response of the second and third storey, where the highest drifts resulted in original conditions. At the same time, very slight differences are observed between RS2 and the other uniform-distribution intervention, RS1, in spite of the fact that the latter incorporates a 25% smaller number of plates in $X$, as a consequence of the greater energy dissipated by the ADAS dampers in this direction.

**Table 7.** Retrofitted conditions—RS3: maximum storey shear and $\rho_S$ values.

| Storey | S1 | S2 | S3 | S4 | S5 | S6 |
|---|---|---|---|---|---|---|
| $V_{xR}$ (kN) | 1996 | 1814 | 1667 | 1696 | 1696 | 1696 |
| $V_{yR}$ (kN) | 2337 | 1912 | 1813 | 1696 | 1696 | 1696 |
| *SDE* | | | | | | |
| $V_x$ (kN) | 1636 | 938 | 638 | 521 | 351 | 52 |
| $V_y$ (kN) | 2028 | 1032 | 818 | 581 | 385 | 121 |
| $\rho_{sx}$ | 0.81 | 0.52 | 0.38 | 0.34 | 0.21 | 0.03 |
| $\rho_{sy}$ | 0.87 | 0.54 | 0.45 | 0.34 | 0.22 | 0.07 |
| *BDE* | | | | | | |
| $V_x$ (kN) | 5058 | 2948 | 2086 | 1659 | 1102 | 136 |
| $V_y$ (kN) | 5222 | 3021 | 2422 | 1722 | 1140 | 354 |
| $\rho_{sx}$ | 2.53 | 1.62 | 1.25 | 0.98 | 0.65 | 0.20 |
| $\rho_{sy}$ | 2.23 | 1.58 | 1.33 | 1.01 | 0.67 | 0.21 |
| *MCE* | | | | | | |
| $V_x$ (kN) | 6222 | 3601 | 2534 | 2055 | 1406 | 162 |
| $V_y$ (kN) | 6578 | 3570 | 2852 | 2015 | 1323 | 384 |
| $\rho_{sx}$ | 3.12 | 1.98 | 1.52 | 1.21 | 0.83 | 0.09 |
| $\rho_{sy}$ | 2.81 | 1.86 | 1.57 | 1.18 | 0.78 | 0.22 |

**Table 8.** Retrofitted conditions—RS3: maximum inter-storey drift and $\rho_u$ values.

| Storey | S1 | S2 | S3 | S4 | S5 | S6 |
|---|---|---|---|---|---|---|
| $u_R$ (mm) | 17.0 | 15.3 | 15.3 | 15.3 | 15.3 | 15.3 |
| *SDE* | | | | | | |
| $u_x$ (mm) | 7.3 | 7.0 | 5.8 | 4.7 | 3.2 | 1.0 |
| $u_y$ (mm) | 8.6 | 8.2 | 6.9 | 5.8 | 4.2 | 2.2 |
| $\rho_{ux}$ | 0.43 | 0.46 | 0.38 | 0.31 | 0.21 | 0.06 |
| $\rho_{uy}$ | 0.50 | 0.53 | 0.45 | 0.38 | 0.27 | 0.14 |
| *BDE* | | | | | | |
| $u_x$ (mm) | 21.7 | 20.8 | 18.3 | 14.6 | 9.3 | 2.6 |
| $u_y$ (mm) | 25.4 | 23.9 | 20.2 | 17.0 | 12.2 | 6.4 |
| $\rho_{ux}$ | 1.27 | 1.36 | 1.19 | 0.95 | 0.60 | 0.17 |
| $\rho_{uy}$ | 1.49 | 1.56 | 1.32 | 1.10 | 0.79 | 0.42 |
| *MCE* | | | | | | |
| $u_x$ (mm) | 26.6 | 25.4 | 22.3 | 17.9 | 11.9 | 3.1 |
| $u_y$ (mm) | 30.6 | 28.7 | 24.3 | 20.4 | 14.7 | 7.6 |
| $\rho_{ux}$ | 1.56 | 1.66 | 1.46 | 1.17 | 0.77 | 0.20 |
| $\rho_{uy}$ | 1.80 | 1.87 | 1.59 | 1.33 | 0.96 | 0.49 |

**Acknowledgements.** Financial support from ReLUIS-DPC Project 2022–2023, Project-WP15: Normative contribution for Isolation and Dissipation, is gratefully acknowledged.

## References

1. Aiken, I.D., Nims, D.K., Whittaker, A.S., Kelly, J.M.: Testing of passive energy dissipation systems. Earthq. Spectra **9**(3), 335–370 (1993)
2. Hanson, R.D., Soong, T.T.: Seismic design with supplemental energy dissipation devices. Publication MNO-8 EERI–Earthquake Engineering Research Center: Oakland, CA (2001)
3. Teruna, D.R., Majid, T.A., Budiono, B.: Experimental study of hysteretic steel damper for energy dissipation capacity. Adv. Civil Eng., Article ID 631726, 12 p (2015). https://doi.org/10.1155/2015/631726
4. Sorace, S., Terenzi, G., Mori, C.: Passive energy dissipation-based retrofit strategies for R/C frame water towers. Eng. Struct. **106**, 385–398 (2016)
5. Terenzi, G.: Energy-based design criterion of dissipative bracing systems for seismic retrofit of framed structures. Appl. Sci. **8**(2), 1–22 (2018)
6. CSI, 2021: SAP2000NL. Theoretical and users' manual, Release 22.03. Computers & Structures Inc., Berkeley, CA, USA (2021)
7. Italian Council of Public Works: NTC 2018 technical standards on constructions [in Italian] Rome, Italy (2018)
8. Gandelli, E., De Domenico, D., Quaglini, V.: Cyclic engagement of hysteretic steel dampers in braced buildings: a parametric investigation. Bull. Earthq. Eng. **19**(12), 5219–5251 (2021). https://doi.org/10.1007/s10518-021-01156-3